科技部奈米科技創新應用計畫

奈米生技醫療

MOST 科技部 Ministry of Science and Technology MOST 110-2124-M-002-010

利用奈米修飾病毒CRISPR/Cas9技術克服非小細胞肺癌EGFR標靶治療之抗藥性 (2/3)

Using nano-modified virus CRISPR/Cas9 to overcome EGFR-TKI resistance in NSCLC (2/3)

Pan-Chyr Yang
Department of Internal Medicine, National Taiwan University College of Medicine, Taipei 10051, Taiwan

Section of CRISPR technology

Therapeutic outcomes of non-small cell lung cancer (NSCLC) have been compromised by an emergence of drug resistance in response to tyrosine kinase inhibitors (TKIs). Herein, we design the recombinant adeno-associated virus serotype 5 (rAAV5) to enable the clustered regularly interspaced short palindromic repeats (CRISPR)-associated 9 ($Cas9^{D10A}$ protein and adenine base editor (ABE) for repairing the mutation of TKIs resistance. NSCLC is re-sensitized by TKIs after infected with rAAV5.

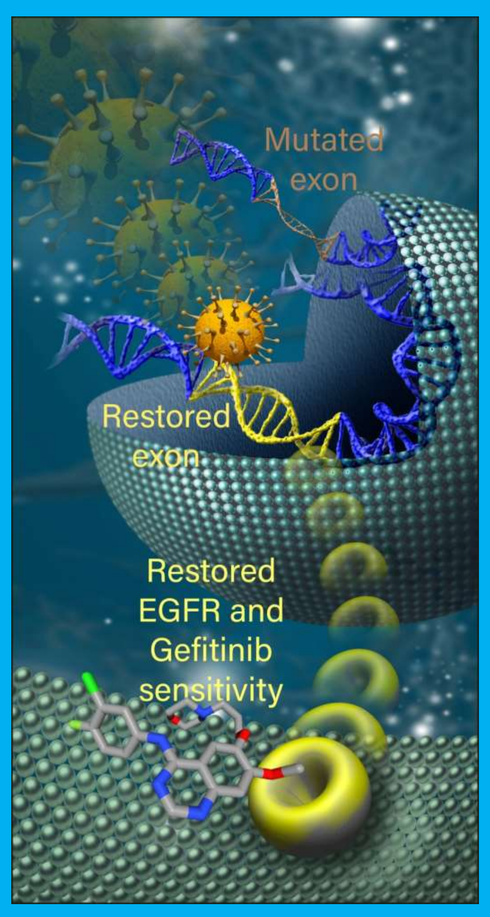

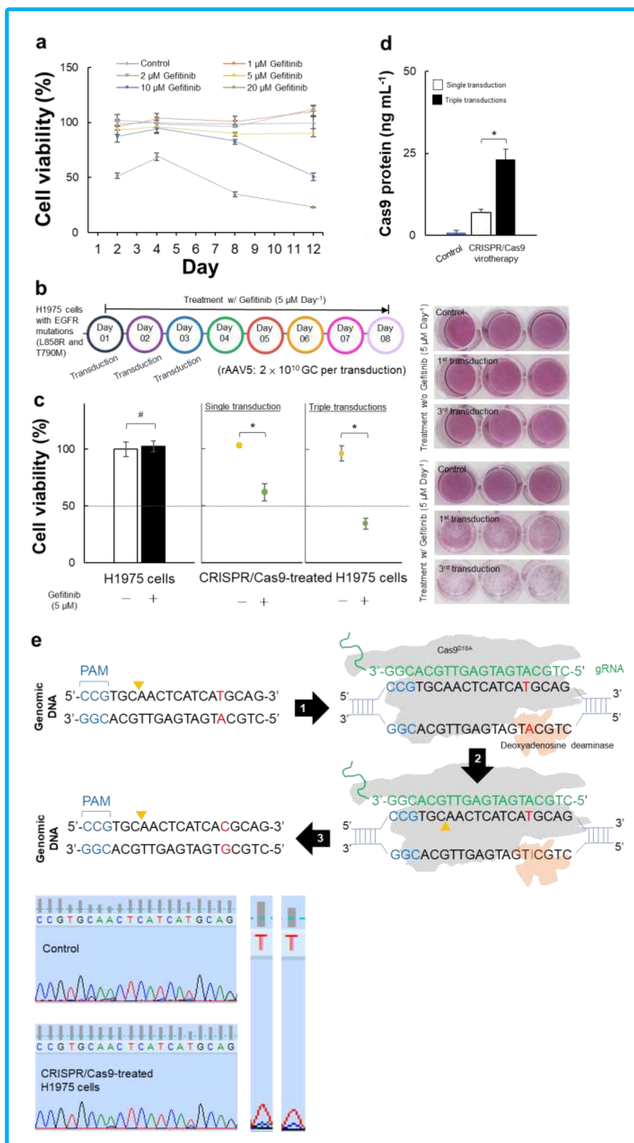

Figure 1. *In vitro* CRISPR/Cas9 virotherapy in NSCLC with EGFR-TKIs resistant. (a) Cell viability of H1975 cells after exposure to various concentration (μM) of Gefitinib over period. Cell viability is given as the percentage of viable cells remaining after treatment for various incubation periods measured by CCK-8 assay and compared against the unexposed. The bars represent the mean ± standard deviation (n = 6). (b) CRISPR/Cas9 treatment protocol for *in vitro* H1975 cells with various transduction conditions. (c) Cell viability of H1975 cells after exposure to various treatments. Cell viability is given as the percentage of viable cells remaining w/o or w/ the CRISPR/Cas9 virotherapy under exposed to Gefitinib measured by the MTS assay and compared against the unexposed (#, $P > 0.5$; *, $P < 0.05$; based on a two-tailed t test, assuming unequal variances). The bars represent the mean ± standard deviation (n = 6). Right panel, pararosaniline-stained photographs of H1975 cells after various treatments. (d) Qualitative determination of Cas9 protein in H1975 cells treated with single or triple transductions (*, $P < 0.05$; based on a two-tailed t test, assuming unequal variances). The bars represent the mean ± standard deviation (n = 6). (e) Schematic diagram of on-target (790, exon 20) adenine conversion mediated by the catalysis activity of an ABE. Step one: genomic DNA binding with $Ca9^{D10A}$ and opening; step two: deamination of target A and nicking of top strand; step three: genomic DNA replication or repair. Lower panel: the target sequences in exon 20 from H1975 cells after CRISPR/Cas9 treatment at Day 8.

Figure 2. *In vivo* CRISPR virotherapy. (a) Treatment protocol for mice with H1975 xenografts treated with various conditions. (b) Tumor weight (mg) or tumor volume (mm^3) of various conditions-treated H1975 ($EGFR^{L858R/T790M}$) xenograft tumors *via* intratumoral injection. Tumor weights of mice were measured at Day 8 (*, $P < 0.05$; based on a two-tailed t test, assuming unequal variances). Tumor sizes were measured by a caliper on the described days (*, $P < 0.05$; based on a two-tailed t test, assuming unequal variances). Bars represent the mean ± standard deviation (n = 5). (c) Representative xenograft NSCLC tumors after various treatments. Bar = 1 cm. (d) Representative images of tumor sections from mice in each group (n = 5) after various treatments at Day 8 were stained with hematoxylin and eosin (H&E), terminal deoxynucleotidyl transferase dUTP nick end labeling (TUNEL) assay (green fluorescence), or DAPI (blue fluorescence). Bars = 500 μm.

Section of nano-carrier design

Approved targeted therapies for NSCLC though initially effective, often eventually fail due to emergence of drug resistance. This evolution is frequently associated with specific driver mutations and greater reliance on aerobic glycolysis, which can increase lactate production in the tumor microenvironment (TME). Meanwhile, oncolytic virotherapy has been approved since 2015, however systemic administration remains particularly challenging and viral delivery for the genome-editing tool of CRISPR system has continued to elicit major concerns due to off targeting. Nevertheless, sophisticated yet robust formulation of viral therapeutics stands to revolutionize their specificity. Notably, physico-chemical properties such as acidosis can regulate viral release and additionally promotes viral transduction. Herein, we report exploitation of NSCLC tumor-secreted lactate in designing an acid-degradable nanoparticle containing the acyclic acetal component of oxidized hyaluronic acid (HA) for release of virus. The virus, lactate oxidase (LOX), and hexanoamide are conjugated with aldehyde-HA through reductive amination. LOX catalyzes the oxidation of lactate to pyruvate, modulating a localized lowering of pH and triggering destabilization of the acyclic component-based nanoparticles. Site-specific delivery is proven by viral transduction in the NSCLC tumor-secreted lactate microenvironment, offering an avenue for improving drug-resistant NSCLC outcomes.

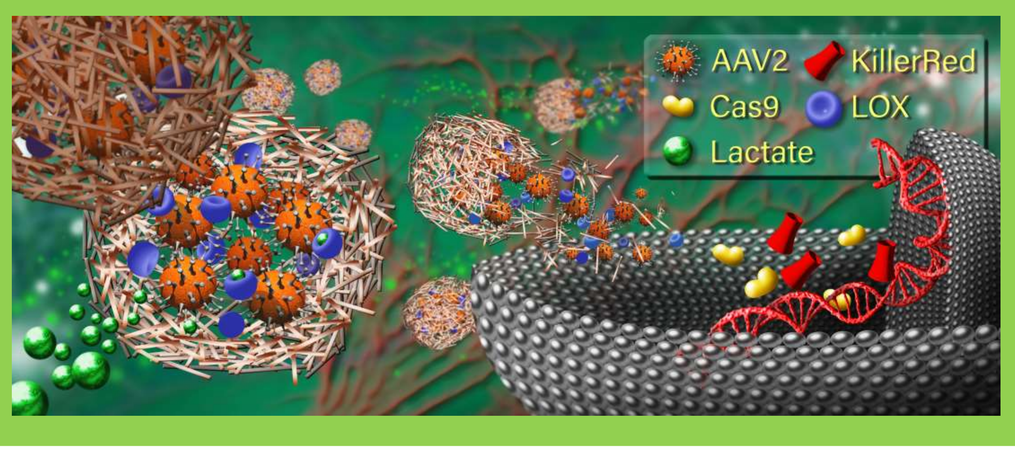

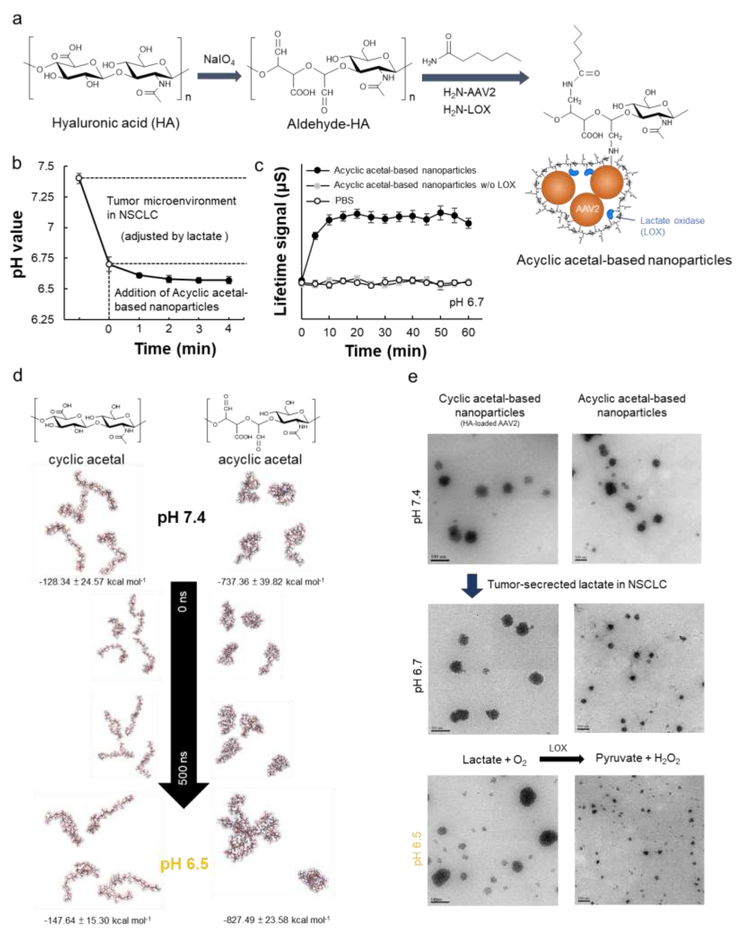

Figure 1. pH-triggered transformation. (a) Scheme preparation of acyclic acetal-based nanoparticles. (b) The pH curve of complete culture medium at pH 6.7 adjusted by lactate (1.0 M) was incubated with the acyclic acetal-based nanoparticles. (c) Phosphorescence lifetime profiles of the different nanoparticles containing an oxygen concentration molecule probe at pH 6.7. Data shows mean of measurements conducted in triplicate ± s.d.. (d) Molecular dynamic (MD) simulations of cyclic acetal of HA or acyclic acetal of HA at neutral pH or acidic pH. Snapshots at different time points presenting the stability of cyclic acetal of HA or acyclic acetal of HA, starting from the initial condition of neutral pH to acidic environment (pH 6.5). (e) TEM image of cyclic acetal-based nanoparticles (HA-loaded AAV2) and acyclic acetal-based nanoparticles at pH 7.4, pH 6.7, or pH 6.5. Bar = 100 nm.